Supplementary Information (SI) for Analytical Methods.
This journal is © The Royal Society of Chemistry 2025

Supplementary information

Specific fluorescence detection strategy for single-stranded nucleic acids by dual-toehold branch migration

Yu Lin,‡[a] Yaxing Xie ,‡[a, b] Guoming Xie,[b] Jianhong Zhang,[a] Ying Yu,[a] Yulei Hou*[a] and Hui Chen*[a]

[a] Department of Laboratory Medicine, The First Affiliated Hospital of Chongqing Medical University, Chongqing, 400016, PR China

[b] Key Laboratory of Medical Diagnostics of Ministry of Education, College of Laboratory Medicine, Chongqing Medical University, Chongqing, 400016, PR China

* Corresponding author:

Yulei Hou: Department of Laboratory Medicine, The First Affiliated Hospital of Chongqing Medical University, No. 1, You Yi Road, Yu-zhong District, Chongqing, 400016, PR China; E-mail: houyulei@cqmu.edu.cn

Hui Chen: Department of Laboratory Medicine, The First Affiliated Hospital of Chongqing Medical University, No. 1, You Yi Road, Yu-zhong District, Chongqing, 400016, PR China; E-mail: huichen@cqmu.edu.cn

‡ Yu Lin and Yaxing Xie are regarded as joint first authors.

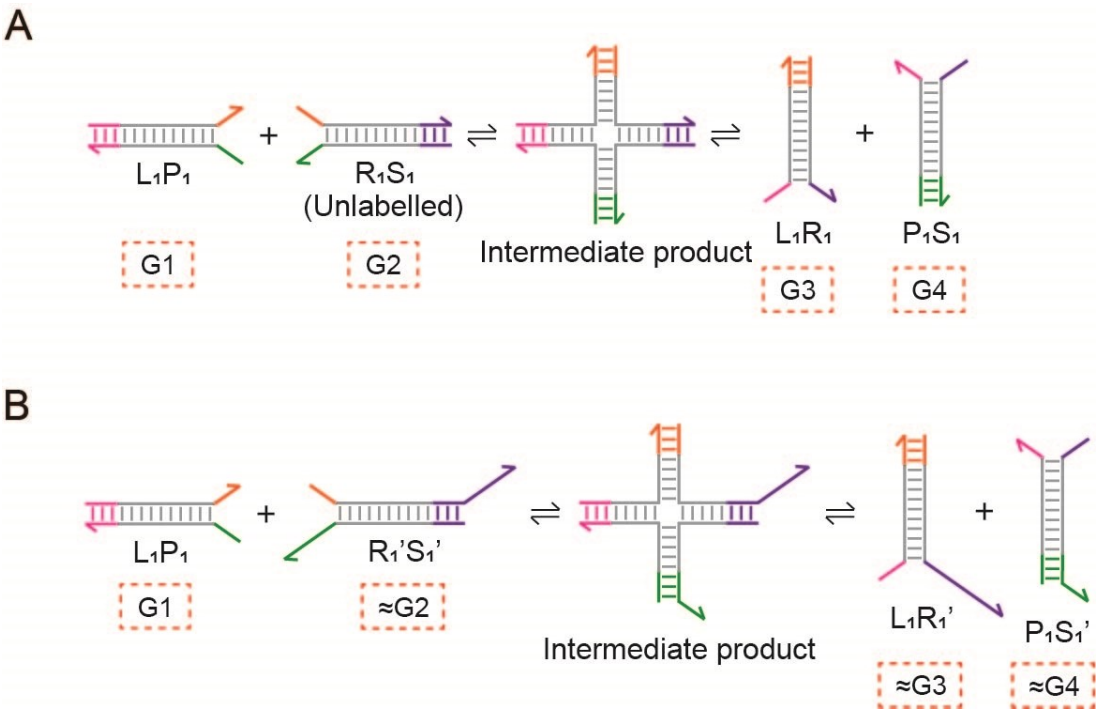

Fig. S1. Reaction process of the PAGE experiment: (A) The DTBM between L_1P_1 and unlabelled R_1S_1. The markers in the red dashed box indicate the theoretical free energy of the double-strand probes in NUPACK at 25 ℃. The free energy and molecular weights of the four double-strand probes (L_1P_1, R_1S_1, L_1R_1 and P_1S_1) are similar. Therefore, the DTBM tends to be a toehold exchange reaction, and the four double probes (L_1P_1, unlabelled R_1S_1, unlabelled L_1R_1 and unlabelled P_1S_1) can coexist in a reaction system. (B) Some unrelated base sequences are added to the ends of R_1S_1, and the newly formed double-strand probe is named R_1'S_1'. Because the unrelated base sequences have little effect on the reaction process (the theoretical free energy of the double-strand probe is still close), the four newly formed double-strand probes (L_1P_1, R_1'S_1', L_1R_1' and P_1S_1') can still coexist in a reaction system, and their molecular weights are each different. In this way, the four newly formed double-strand probes can be distinguished in one lane on the image of PAGE.

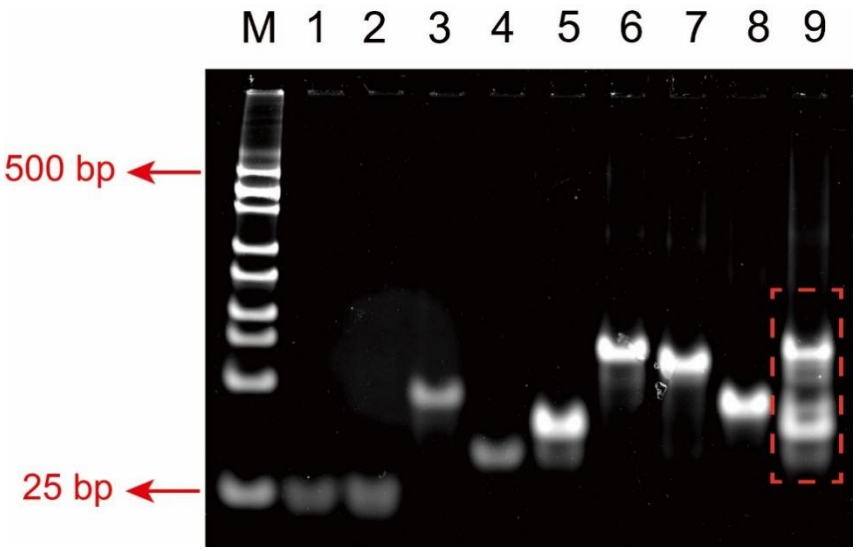

Fig. S2. PAGE image of the DTBM between L_1P_1 and $R_{1\text{-}1}$'$S_{1\text{-}1}$'. Lane M: DNA marker; lane 1: L_1 (1 μM); lane 2: P_1 (1 μM); lane 3: $R_{1\text{-}1}$' (1 μM); lane 4: $S_{1\text{-}1}$' (1 μM); lane 5: L_1P_1 (750 nM); lane 6: $R_{1\text{-}1}$'$S_{1\text{-}1}$' (750 nM); lane 7: L_1 $R_{1\text{-}1}$' (750 nM); lane 8: P_1 $S_{1\text{-}1}$' (750 nM); lane 9: L_1P_1 (750 nM) + $R_{1\text{-}1}$'$S_{1\text{-}1}$' (750 nM).

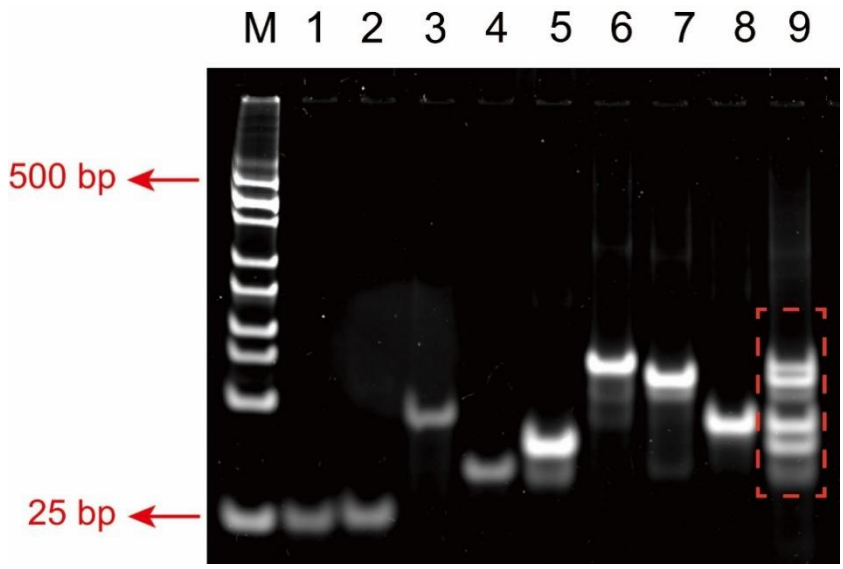

Fig. S3. PAGE image of the DTBM between L_1P_1 and $R_{1\text{-}2}$'$S_{1\text{-}1}$'. Lane M: DNA marker; lane 1: L_1 (1 μM); lane 2: P_1 (1 μM); lane 3: $R_{1\text{-}2}$' (1 μM); lane 4: $S_{1\text{-}1}$' (1 μM); lane 5: L_1P_1 (750 nM); lane 6: $R_{1\text{-}2}$'$S_{1\text{-}1}$' (750 nM); lane 7: L_1 $R_{1\text{-}2}$' (750 nM); lane 8: P_1 $S_{1\text{-}1}$' (750 nM); lane 9: L_1P_1 (750 nM) + $R_{1\text{-}2}$'$S_{1\text{-}1}$' (750 nM).

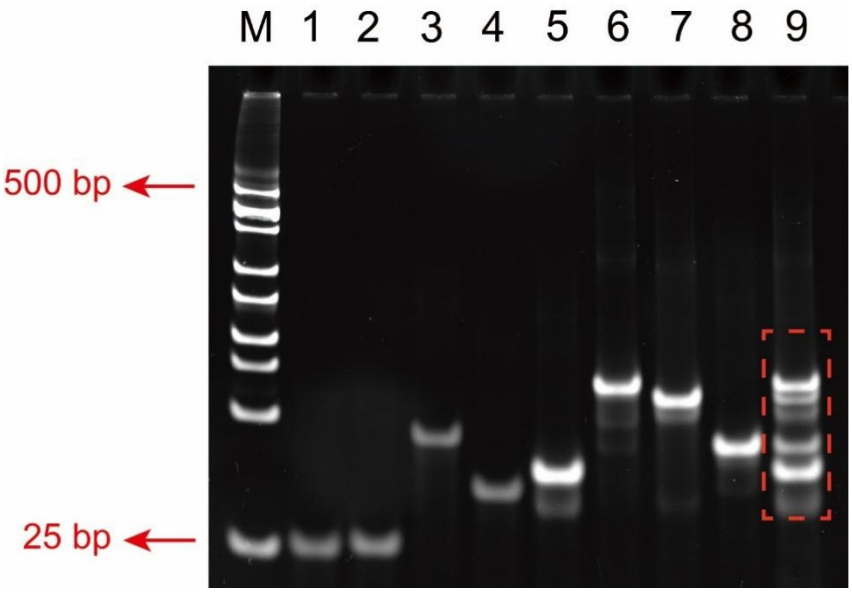

Fig. S4. PAGE image of the DTBM between L_1P_1 and $R_{1\text{-}3}$'$S_{1\text{-}3}$'. Lane M: DNA marker; lane 1: L_1 (1 μM); lane 2: P_1 (1 μM); lane 3: $R_{1\text{-}3}$' (1 μM); lane 4: $S_{1\text{-}3}$' (1 μM); lane 5: L_1P_1 (750 nM); lane 6: $R_{1\text{-}3}$'$S_{1\text{-}3}$' (750 nM); lane 7: L_1 $R_{1\text{-}3}$' (750 nM); lane 8: P_1 $S_{1\text{-}3}$' (750 nM); lane 9: L_1P_1 (750 nM) + $R_{1\text{-}3}$'$S_{1\text{-}3}$' (750 nM).

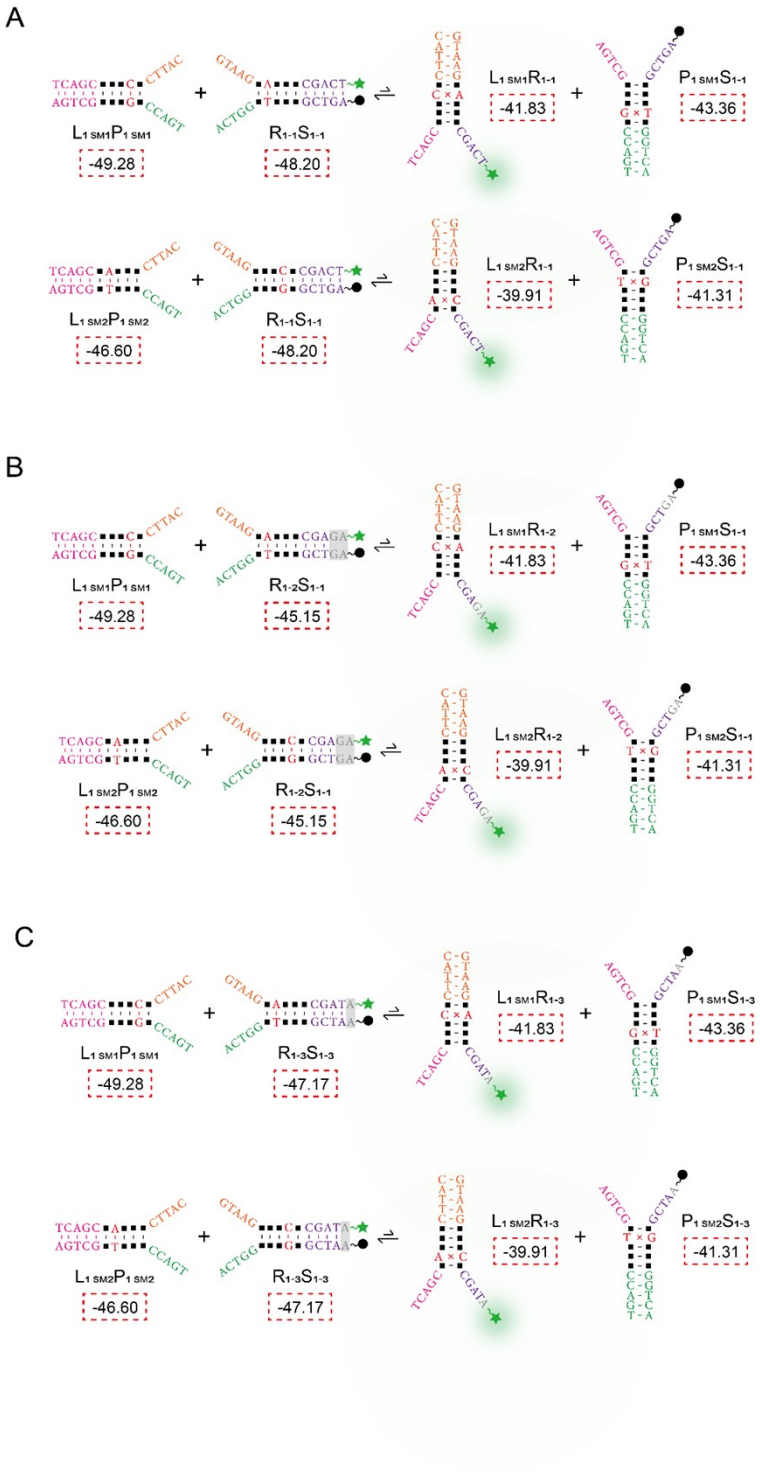

Fig. S5. Reaction process of the DTBM in two groups of mutant sequences ($L_{1\ SM1}P_{1\ SM1}$ and $L_{1\ SM2}P_{1\ SM2}$) and three R_1S_1 sequences: (A) two groups of mutant sequences and $R_{1\text{-}1}S_{1\text{-}1}$. (B) two groups of mutant sequences and $R_{1\text{-}2}S_{1\text{-}1}$. (C) two groups of mutant sequences and $R_{1\text{-}3}S_{1\text{-}3}$. The numbers in the red dashed box indicate the theoretical free energy of the double-strand probes in NUPACK at 25 ℃.

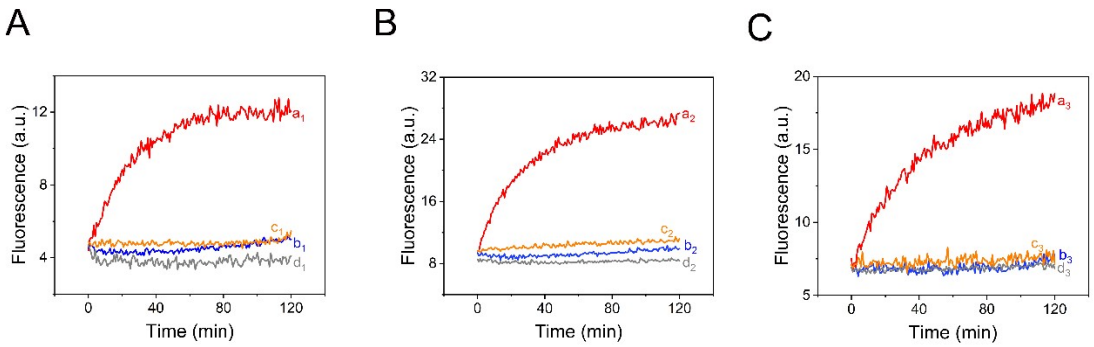

Fig. S6. Time-dependent fluorescence curves of the DTBM between L_1P_1 and different R_1S_1 sequences. (A) L_1P_1 and $R_{1\text{-}1}S_{1\text{-}1}$, (B) L_1P_1 and $R_{1\text{-}2}S_{1\text{-}1}$, (C) L_1P_1 and $R_{1\text{-}3}S_{1\text{-}3}$. The red (a1-a3), blue (b1-b3), and orange (c1-c3) curves represent mixtures of 25 nM L_1P_1, $L_{1\ SM1}P_{1\ SM1}$, and $L_{1\ SM2}P_{1\ SM2}$, respectively, each mixed with 500 nM R_1S_1 probes. The gray curves (d1-d3) represent the background signals of 500 nM R_1S_1 probes.

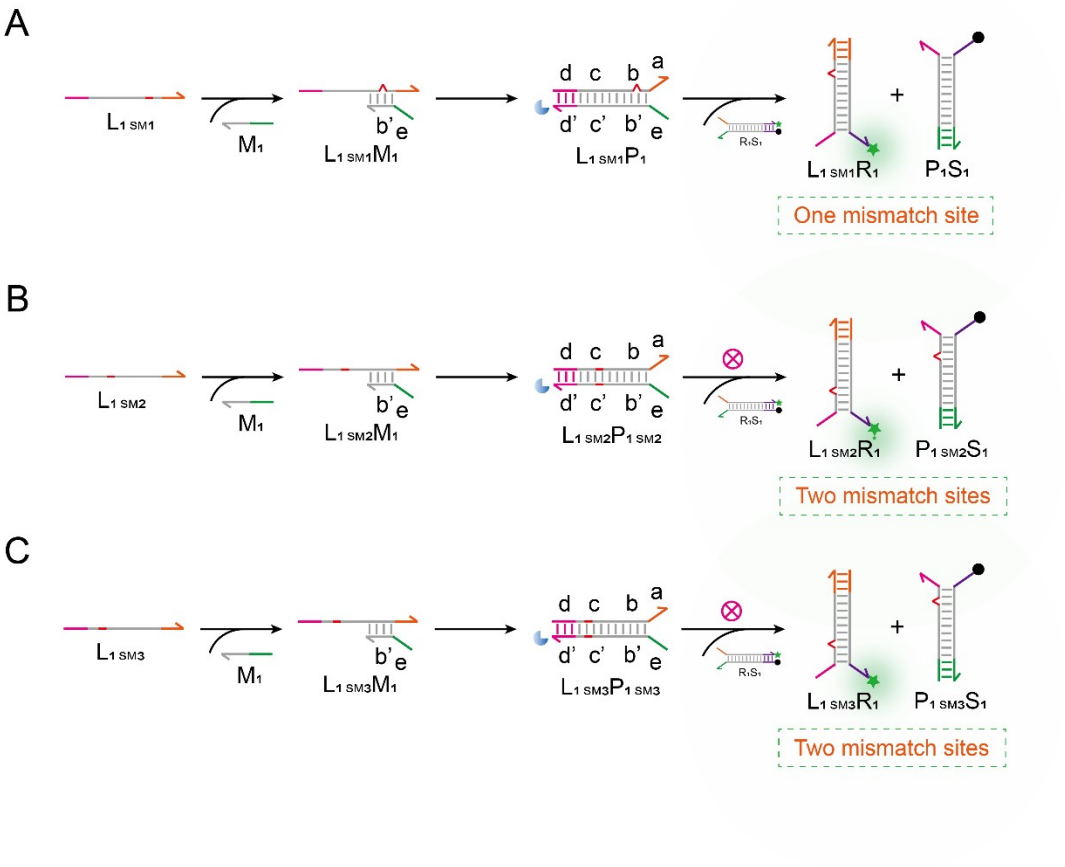

Fig. S7. Reaction process of the DTBM between mutant L_1P_1 and R_1S_1: (A) $L_{1\ SM1}P_1$ and R_1S_1. The mismatch site is located in region b of $L_{1\ SM1}$, and there is one mismatch site in $L_{1\ SM1}R_1$. (B) $L_{1\ SM2}P_{1\ SM2}$ and R_1S_1. The mismatch site is located in region c of $L_{1\ SM2}$, and there are two mismatch sites in $L_{1\ SM2}R_1$ and $P_{1\ SM2}S_1$. (C) $L_{1\ SM3}P_{1\ SM3}$ and R_1S_1. The mismatch site is located in region c of $L_{1\ SM3}$, and there are two mismatch sites in $L_{1\ SM2}R_1$ and $P_{1\ SM2}S_1$.

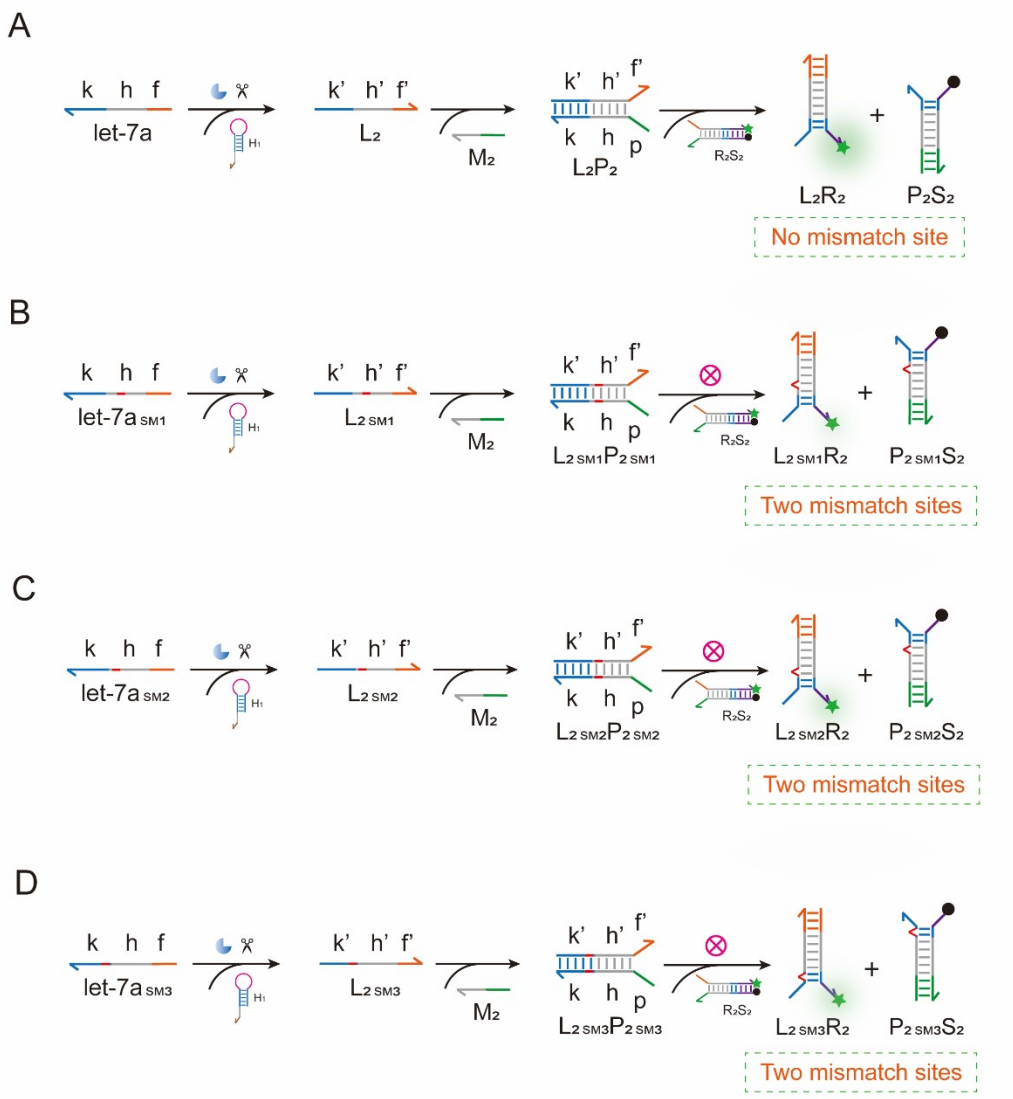

Fig. S8. The SDA-DTBM reaction between R_2S_2 and L_2P_2 as well as mutants : (A) L_2P_2 and R_2S_2. (B) $L_{2\ SM1}P_{2\ SM1}$ and R_2S_2. The mismatch site is located in the h region of let-7a $_{SM1}$, and there are two mismatch sites in $L_{2\ SM1}R_2$ and $P_{2\ SM1}S_2$. (C) $L_{2\ SM2}P_{2\ SM2}$ and R_2S_2. The mismatch site is located in the h region of let-7a $_{SM2}$, and there are two mismatch sites in $L_{2\ SM2}R_2$ and $P_{2\ SM2}S_2$. (D) $L_{2\ SM3}P_{2\ SM3}$ and R_2S_2. The mismatch site is located in the k region of let-7a $_{SM3}$, and there are two mismatch sites in $L_{2\ SM3}R_2$ and $P_{2\ SM3}S_2$.

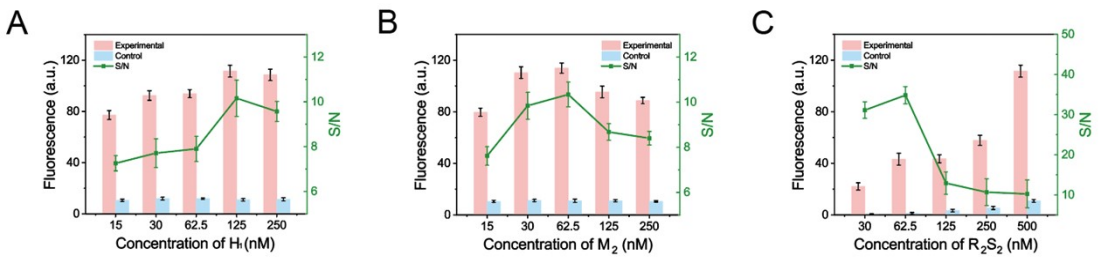

Fig. S9. Optimization of the concentration of the probes in the SDA-triggered DTBM system: (A) Optimization of the concentration of H_1, (B) Optimization of the concentration of M_2, and (C) Optimization of the concentration of R_2S_2. The experimental groups represent the fluorescence signal values in the presence of 30 nM let-7a, and the control groups represent the fluorescence signal values in the absence of let-7a. S/N represents the ratio of the measured values of the experimental group and the control group.

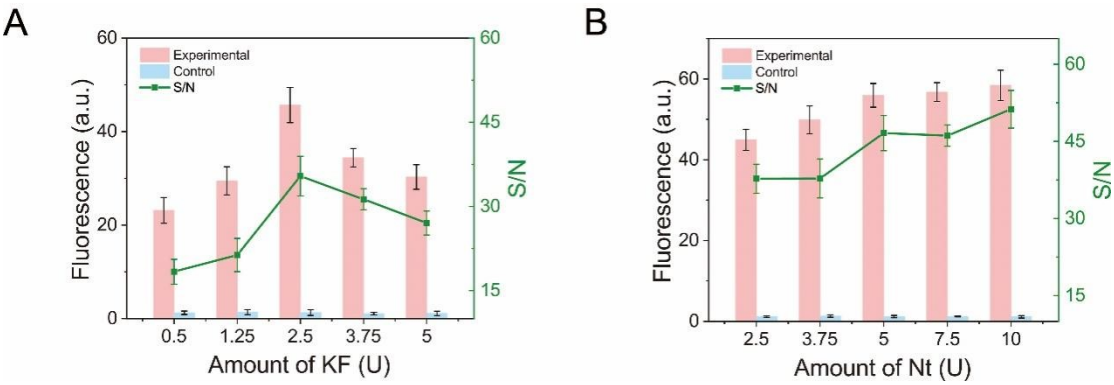

Fig. S10. Optimization of the amounts of KF and Nt in the SDA-triggered DTBM system: (A) Optimization of the amount of KF, and (B) Optimization of the amount of Nt. The experimental groups represent the fluorescence signal values in the presence of 30 nM let-7a, and the control groups represent the fluorescence signal values in the absence of let-7a. S/N represents the ratio of the measured values of the experimental group and the control group.

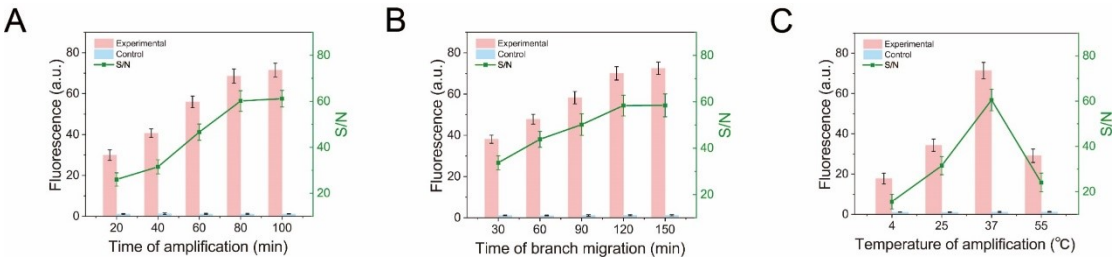

Fig. S11. Optimization of the reaction time and temperature in the SDA-triggered DTBM system: (A) Optimization of the time of amplification, (B) Optimization of the time of branch migration, and (C) Optimization of the temperature of amplification. The experimental groups represent the fluorescence signal values in the presence of 30 nM let-7a, and the control groups represent the fluorescence signal values in the absence of let-7a. S/N represents the ratio of the measured values of the experimental group and the control group.

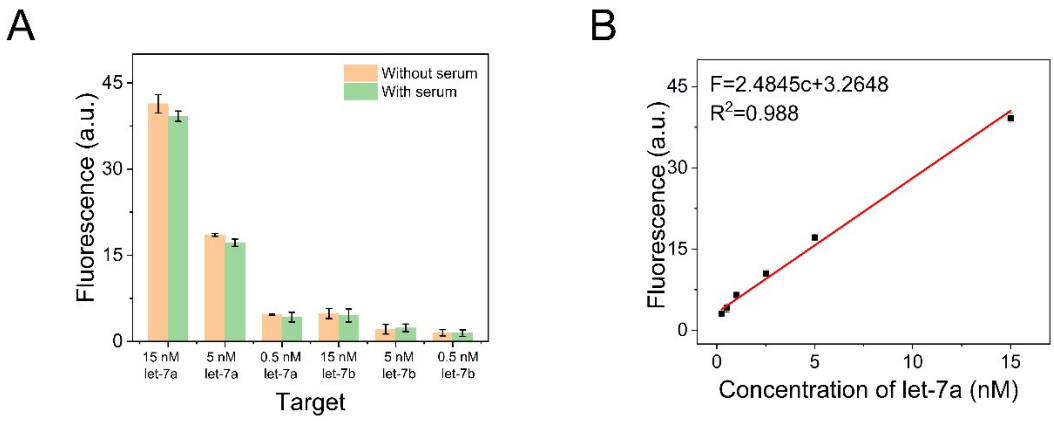

Fig. S12. (A) The fluorescence of different concentrations of let-7a and let-7b in the SDA-triggered DTBM reaction system with or without the 5-fold diluted serum system. (B) The linear relationship between the fluorescence signal value and the concentration of let-7a ranged from 0.25 nM to 15 nM in the 5-fold diluted serum system (n=3).

Table S1. The oligonucleotides used in the experiment.

No.	Sequence (5' to 3')
L_1	TCAGCAGATTCGCACAGTCCAGGGTTAGCTTAC
$L_{1\ SM1}$	TCAGCAGATTCGCACAGTCCAGGGCTAGCTTAC
$L_{1\ SM2}$	TCAGCAGATTGGCACAGTCCAGGGTTAGCTTAC
M_1	TGACCCTAACCCTGG
P_1	TGACCCTAACCCTGGACTGTGCGAATCTGCTGA
$P_{1\ SM1}$	TGACCCTAGCCCTGGACTGTGCGAATCTGCTGA
$P_{1\ SM2}$	TGACCCTAACCCTGGACTGTGCCAATCTGCTGA
$R_{1\text{-}1}$	GTAAGCTAACCCTGGACTGTGCGAATCTCGACT-FAM
$S_{1\text{-}1}$	BHQ-1-AGTCGAGATTCGCACAGTCCAGGGTTAGGGTCA
$R_{1\text{-}2}$	GTAAGCTAACCCTGGACTGTGCGAATCTCGAGA-FAM
$R_{1\text{-}3}$	GTAAGCTAACCCTGGACTGTGCGAATCTCGATA-FAM
$S_{1\text{-}3}$	BHQ-1-AATCGAGATTCGCACAGTCCAGGGTTAGGGTCA
$R_{1\text{-}1}$'	GTAAGCTAACCCTGGACTGTGCGAATCTCGACTCAACAACAAC AACAACAACA
$S_{1\text{-}1}$'	AGTCGAGATTCGCACAGTCCAGGGTTAGGGTCACAACAACAAC
$R_{1\text{-}2}$'	GTAAGCTAACCCTGGACTGTGCGAATCTCGAGACAACAACAAC AACAACAACA
$R_{1\text{-}3}$'	GTAAGCTAACCCTGGACTGTGCGAATCTCGATACAACAACAAC AACAACAACA
$S_{1\text{-}3}$'	AATCGAGATTCGCACAGTCCAGGGTTAGGGTCACAACAACAAC
let-7a	UGAGGUAGUAGGUUGUAUAGUU
H	TATAGTTGTCTCTAACTATACAACCAAAA
L_2	AACTATACAACCTACTACCTCA
P_2	ACTCGTAGTAGGTTGTATAGTT

M_2	ACTCGTAGTAGG
R_2	TGAGGTAGTAGGTTGTATTCAA-FAM
S_2	BHQ-1-TTGAATACAACCTACTACGAGT
let-7a $_{SM1}$	UGAGGUAGUAGGUGGUAUAGUU
let-7a $_{SM2}$	UGAGGUAGUAGGUUAUAUAGUU
let-7a $_{SM3}$	UGAGGUAGUAGGUUGGAUAGUU
let-7b	UGAGGUAGUAGGUUGUGUGGUU
let-7d	AGAGGUAGUAGGUUGCAUAGUU
miRNA-21	UAGCUUAUCAGACUGAUGUUGA
miRNA-155	UUAAUGCUAAUCGUGAUAGGGGUU
$L_{2\ SM1}$	AACTATACCACCTACTACCTCA
$L_{2\ SM2}$	AACTATATAACCTACTACCTCA
$L_{2\ SM3}$	AACTATCCAACCTACTACCTCA
$L_{2\ 7b}$	AACCACACAACCTACTACCTCA
$L_{2\ 7d}$	AACTATGCAACCTACTACCTCT
$P_{2\ SM1}$	ACTCGTAGTAGGTGGTATAGTT
$P_{2\ SM2}$	ACTCGTAGTAGGTTATATAGTT
$P_{2\ SM3}$	ACTCGTAGTAGGTTGGATAGTT
$P_{2\ 7b}$	ACTCGTAGTAGGTTGTGTGGTT
$P_{2\ 7d}$	TCTCGTAGTAGGTTGCATAGTT

Note:

[1] The red markers indicate the mutantion site or the various bases from let-7 miRNA family.

[2] The blue markers indicate the recognition site of the Nt. BsmAI.

Table S2. The theoretical free energy and the △G of the double-strand probes of three R_1S_1 sequences in NUPACK at 25 ℃.

the double-stranded probes	Free energy (kcal/mol)	the double-stranded probes	Free energy (kcal/mol)	the double-stranded probes	Free energy (kcal/mol)
L_1P_1	-48.19	L_1P_1	-48.19	L_1P_1	-48.19
$R_{1\text{-}1}S_{1\text{-}1}$	-48.20	$R_{1\text{-}2}S_{1\text{-}1}$	-45.15	$R_{1\text{-}3}S_{1\text{-}3}$	-47.17
$L_1R_{1\text{-}1}$	-46.16	$L_1R_{1\text{-}2}$	-46.16	$L_1R_{1\text{-}3}$	-46.16
$P_1S_{1\text{-}1}$	-48.26	$P_1S_{1\text{-}1}$	-48.26	$P_1S_{1\text{-}3}$	-48.26
△G	1.97	△G	-1.08	△G	0.94
L_1P_1	-48.19	L_1P_1	-48.19	L_1P_1	-48.19
$R_{1\text{-}1}$'$S_{1\text{-}1}$'	-48.71	$R_{1\text{-}2}$'$S_{1\text{-}1}$'	-45.56	$R_{1\text{-}3}$'$S_{1\text{-}3}$'	-47.58
$L_1R_{1\text{-}1}$'	-46.16	$L_1R_{1\text{-}2}$'	-46.16	$L_1R_{1\text{-}3}$'	-46.16
$P_1S_{1\text{-}1}$'	-48.26	$P_1S_{1\text{-}1}$'	-48.26	$P_1S_{1\text{-}3}$'	-48.26
△G	2.48	△G	-0.67	△G	1.35
$R_{1\text{-}1}S_{1\text{-}1}$	-48.20	$R_{1\text{-}2}S_{1\text{-}1}$	-45.15	$R_{1\text{-}3}S_{1\text{-}3}$	-47.17
$L_{1\ SM1}P_{1\ SM1}$	-49.28	$L_{1\ SM1}P_{1\ SM1}$	-49.28	$L_{1\ SM1}P_{1\ SM1}$	-49.28
$L_{1\ SM1}R_{1\text{-}1}$	-41.83	$L_{1\ SM1}R_{1\text{-}2}$	-41.83	$L_{1\ SM1}R_{1\text{-}3}$	-41.83
$P_{1\ SM1}S_{1\text{-}1}$	-43.36	$P_{1\ SM1}S_{1\text{-}1}$	-43.36	$P_{1\ SM1}S_{1\text{-}3}$	-43.36
△G	12.29	△G	9.24	△G	11.26
$R_{1\text{-}1}S_{1\text{-}1}$	-48.20	$R_{1\text{-}2}S_{1\text{-}1}$	-45.15	$R_{1\text{-}3}S_{1\text{-}3}$	-47.17
$L_{1\ SM2}P_{1\ SM2}$	-47.93	$L_{1\ SM2}P_{1\ SM2}$	-47.93	$L_{1\ SM2}P_{1\ SM2}$	-47.93
$L_{1\ SM2}R_{1\text{-}1}$	-41.91	$L_{1\ SM2}R_{1\text{-}2}$	-41.91	$L_{1\ SM2}R_{1\text{-}3}$	-41.91
$P_{1\ SM2}S_{1\text{-}1}$	-42.33	$P_{1\ SM2}S_{1\text{-}1}$	-42.33	$P_{1\ SM2}S_{1\text{-}3}$	-42.33
△G	11.89	△G	8.84	△G	10.86

Note: the left two columns correspond to the $R_{1\text{-}1}S_{1\text{-}1}$ sequence, the middle two columns correspond to the $R_{1\text{-}2}S_{1\text{-}1}$ sequence, and the right two columns correspond to the $R_{1\text{-}3}S_{1\text{-}3}$ sequence. The red markers indicate △G at different mutation sites. For the fluorescence labelled sequences, the influence of fluorophores is ignored.

Table S3. The theoretical free energy of the double-strand probes in the detection of let-7a at 25 ℃.

the double-stranded probes	Free energy (kcal/mol)	the double-stranded probes	Free energy (kcal/mol)	the double-stranded probes	Free energy (kcal/mol)
L_2P_2	-25.64	$L_{2\ SM1}P_{2\ SM1}$	-26.45	$L_{2\ SM2}P_{2\ SM2}$	-24.17
R_2S_2	-26.11	R_2S_2	-26.11	R_2S_2	-26.11
L_2R_2	-27.72	$L_{2\ SM1}R_2$	-23.41	$L_{2\ SM2}R_2$	-22.57
P_2S_2	-27.92	$P_{2\ SM1}S_2$	-24.10	$P_{2\ SM2}S_2$	-22.52
△G	-3.89	△G	5.14	△G	5.19
$L_{2\ SM3}P_{2\ SM3}$	-26.74	$L_{2\ 7b}P_{2\ 7b}$	-28.55	$L_{2\ 7d}P_{2\ 7d}$	-27.35
R_2S_2	-26.11	R_2S_2	-26.11	R_2S_2	-26.11
$L_{2\ SM3}R_2$	-24.18	$L_{2\ 7b}R_2$	-25.54	$L_{2\ 7d}R_2$	-24.10
$P_{2\ SM3}S_2$	-25.42	$P_{2\ 7b}S_2$	-26.35	$P_{2\ 7d}S_2$	-24.38
△G	3.25	△G	2.77	△G	4.98

Note: the black markers correspond to the double-strand probes generated by let-7a, the blue markers correspond to the double-strand probes generated by the let-7a mismatch targets, and the orange markers correspond to the double-strand probes generated by the let-7 miRNA family. The red markers indicate △G at mutations and miRNAs. For the fluorescence labelled sequences, the influence of fluorophores is ignored.

Table S4. Comparison of the present method with recently reported methods for miRNA detection.

Method	Target	LOD	Specificity	Ref
Microfluidics	let-7a	100 pM	high	[1]
Electrochemistry	let-7a	0.25 nM	moderate	[2]
Colorimetric	let-7a	63.2 pM	high	[3]
Fluorescent	miRNA-156	1.0 nM	high	[4]
Atomic force microscope	miRNA-203 and miRNA-205	95nM and 97nM	general	[5]
Electrochemistry	let-7a	48 pM	high	[6]
SDA-DTBM	ssDNA and let-7a	1.88 nM for ssDNA and 113 pM for let-7a	excellent with DFs (24.49 and 30.59)	This work

Table S5. Recovery test for the detection of let-7a in the 5-fold diluted serum samples.

No.	Added (nM)	Detected (nM) (n=3)	Recovery (%)	RSD (%) (n=3)
1	0.5	0.53	105.34	4.73
2	5	5.18	103.60	3.56
3	15	14.46	96.40	2.03

[1] Y. Lu, J. Xu, S. Liu, B. Tian and F. Long, Mikrochim Acta, 2024, 192, 9.
[2] J. Wu, W. Lv, Q. Yang, H. Li and F. Li, Biosens Bioelectron, 2021, 171, 112707.
[3] H. Xu, F. Yang, D. Chen, W. Ye, G. Xue and L. Jia, iScience, 2023, 26, 106331.
[4] L. Chen, G. Hu, B. Cui, J. Gao, X. Gu, H. Cui and Z. Zeng, Sensors and Actuators B-Chemical, 2024, 404.
[5] M. A. Andrade, L. F. Rodrigues, J. C. M. Ierich, M. E. Melendez, A. L. Carvalho, A. C. de Carvalho, C. Steffens, F. C. Abdalla, O. N. Oliveira, Jr. and F. L. Leite, Ieee Sensors Journal, 2020, 20, 2860-2867.
[6] L. L. Wang, T. T. Shan, L. Pu, J. Zhang, R. Hu, Y. H. Yang, J. M. Yang and Y. Zhao, Microchimica Acta, 2022, 189.